Electromagnetic Response of Three-Dimensional Topological Crystalline Insulators

Srinidhi T. Ramamurthy, Yuxuan Wang, and Taylor L. Hughes

Phys. Rev. Lett. **118**, 146602 — Published 3 April 2017

DOI: 10.1103/PhysRevLett.118.146602

Electromagnetic Response of Three-dimensional Topological Crystalline Insulators

Srinidhi T. Ramamurthy, Yuxuan Wang, and Taylor L. Hughes
Department of Physics, Institute for Condensed Matter Theory, University of Illinois at Urbana-Champaign, IL 61801, USA

Topological crystalline insulators (TCI) are a new class of materials which have metallic surface states on select surfaces due to point group crystalline symmetries. In this letter, we consider a model for a three-dimensional (3D) topological crystalline insulator with Dirac nodes occurring on a surface that are protected by the mirror and time reversal symmetry. We demonstrate that the electromagnetic response for such a system is characterized by a 1-form b_μ. b_μ can be inferred from the locations of the surface Dirac nodes in energy-momentum space. From both the effective action and analytical band structure calculations, we show that the vortex core of $\vec{b}$ or a domain wall of a component of $\vec{b}$ can trap surface charges.

Topological phases of matter have been at the forefront of condensed matter physics for the past decade. One reason for the excitement is that topological phases can exhibit electromagnetic responses that display their topological nature. The integer quantum Hall (IQH) effect was the first such system, and its quantized Hall conductance is characterized by a topological integer [1] multiplying the conductance quantum e^2/h. In recent years, the ten-fold, periodic table classification of electronic topological insulators and superconductors with time-reversal (TR) $\mathcal{T}$, particle-hole (PH) $\mathcal{C}$, and/or chiral symmetry $\mathcal{S}$ was completed in Refs. [2–4], and ushered in the concept of a symmetry protected topological (SPT) phase. The electromagnetic (EM) response theories of many of the topological insulator (TI) phases were developed in Ref. [3], and extended from what was known about the IQH to all fermionic SPTs. For example, the 3D $\mathcal{T}$-invariant topological insulator has an odd number of Dirac cones on each surface, and harbors a half quantum Hall effect when $\mathcal{T}$ is broken on the surface. An odd number of Dirac cones, and the corresponding Hall effect, can never occur in a purely 2D system with the same symmetries without interactions. Indeed, the surface quantum Hall effect is actually a signature of a *bulk* EM response: the topological magneto-electric effect[3, 5, 6] with a response coefficient determined by a $\mathbb{Z}_2$ topological invariant[3].

After the periodic table was complete, and after many exciting materials predictions and discoveries[7–14], the classification of topological crystalline phases (TCIs) with point/space-group symmetries, such as reflection and discrete rotation, was initiated and continues to be an active area of research[15–31]. One highlight of this line of research was the prediction and experimental confirmation of a 3D TCI phase in PbSnTe[32–35]. The topological properties of this system are protected by mirror symmetry, and it exhibits an insulating bulk with an even number of symmetry-protected Dirac-cone surface states on mirror-symmetric surfaces. The goal of this article is to predict a characteristic electromagnetic response property that can be observed in PbSnTe and similar 3D TCIs protected by mirror symmetry (mTCIs).

Three-dimensional mTCIs are characterized by integer invariants: the mirror Chern numbers C_M[16]. To define and illustrate the consequences of the C_M let us consider a system with mirror symmetry $\mathcal{M}_z$ in the z-direction with $\mathcal{M}_z^2 = -1$. We can label eigenstates in the $k_z = 0$ and $k_z = \pi$ planes of the Brillouin zone (BZ) with the eigenvalues $\pm i$ of $\mathcal{M}_z$, and this allows one to define mirror Chern numbers $C_M(\Lambda) = \frac{C_{+i}(\Lambda) - C_{-i}(\Lambda)}{2}$, where $C_{\pm i}(\Lambda)$ is the usual Chern number of each mirror sector in the plane $\Lambda = 0, \pi$. When a C_M is non-vanishing, then, on mirror-invariant surfaces, say one normal to $\hat{x}$, there will be Dirac cones protected by the mirror symmetry. Furthermore, these cones lie in mirror invariant lines in the surface BZ projected from the corresponding Λ planes. The number of *stable* Dirac cones on each mirror line is given by $C_M(\Lambda)$[16]. If we allow for broken translation symmetry, then the total number of stable surface cones is $\mathcal{C}_M \equiv C_M(\Lambda_1) + C_M(\Lambda_2)$. We illustrate the case with $C_M(0) = 2, C_M(\pi) = 0$ in Fig. 1 where we have two stable Dirac nodes on the surface perpendicular to $\hat{x}$ on the $k_z = 0$ plane.

In this article we will show that mTCIs have a robust electromagnetic (EM) response that is determined by both a topological property (the existence of stable surface states determined by $\mathcal{C}_M$), and a geometrical property (the momentum and energy locations of the surface nodes). To show this, we first provide a lattice model for a mTCI built from two copies of a 3D time-reversal invariant TI on a cubic lattice. By itself, this system has a trivial topological magnetoelectric effect, but when coupled to a field b_μ which preserves the mirror symmetry, yet splits the surface Dirac nodes in energy-momentum space, an additional EM response is generated. In this article we only consider systems which also retain $\mathcal{T}$ symmetry since the experimentally realized mTCIs have $\mathcal{T}$-symmetry, and it will simplify some discussions.

For the simplest case with $\mathcal{C}_M = 2$, and with $\mathcal{T}$-symmetry, we can obtain a response theory of the mTCI via analogy with the 3D TI. In the continuum limit, the field b_μ in which we are interested couples to the theory

precisely as a valley gauge field for the two species of surface Dirac cones/valleys. By performing a diagrammatic calculation in the continuum limit, we find that the effective response action is given by:

$$\mathcal{S}_{\rm TCI}[A,b] = \frac{e}{8\pi^2}\int \mathrm{d}^4x\, \epsilon^{\mu\nu\rho\sigma}\Theta f_{\mu\nu}F_{\rho\sigma}, \qquad (1)$$

where $\Theta = \pi$ inside the bulk of the mTCI, and $f_{\mu\nu}, F_{\mu\nu}$ are the field-strengths of b_μ and A_μ. The surface of the mTCI, can be thought of as a domain wall of Θ from π to 0, and Eq. (1) implies a surface response $S_{2D}[A,b] = \frac{e}{4\pi}\int_{\rm surf} d^3x\epsilon^{\mu\nu\rho}b_\mu\partial_\nu A_\rho$ bound to the Θ domain wall. This surface response matches an EM response of a 2D Dirac semi-metal (DSM) with broken inversion symmetry if we identify b_μ with the energy/momentum separation of the Dirac node valleys[36, 37]. This might have been anticipated, since the even number of Dirac nodes on the surface of the mTCI is similar to the electronic structure of a 2D DSM. However, we find precisely half the coefficient that would occur in a 2D DSM with mirror and $\mathcal{T}$ ($\mathcal{T}^2 = -1$) symmetries, which makes it anomalous. Ultimately, the EM response of the mTCI implies localized charge and/or current density bound at defects in the b_μ field on the surface. To verify the validity of the result Eq. (1) obtained in the continuum limit, we explicitly calculate the microscopic origin of the response from a lattice model bound state calculation. Finally, we discuss experimental proposals and predictions.

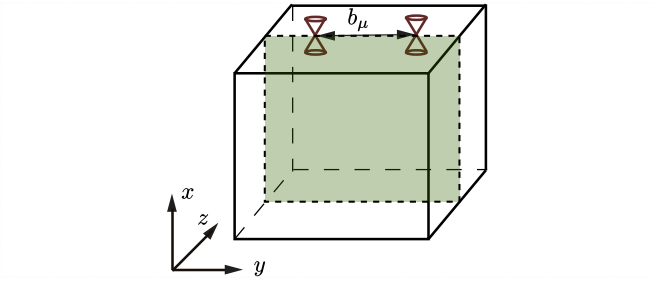

FIG. 1. An illustration of a topological crystalline insulator in 3D with two surface Dirac cones localized on the surface perpendicular to the x-direction. $b_\mu = (b_0, b_y)$ is the energy-momentum separation of the Dirac nodes. For the model that we construct, the Dirac nodes are stabilized by $\mathcal{M}_z$ symmetry. We show the mirror plane in the bulk, and mirror lines on the surfaces by the green rectangle and its dashed boundary.

Lattice Model for TCI.— Let us begin with the lattice Hamiltonian for a single copy of TI given by[3]:

$$H_{\rm TI} = \sin k_x\Gamma^x + \sin k_y\Gamma^y + \sin k_z\Gamma^z - m(k_x,k_y,k_z)\Gamma^0, \qquad (2)$$

where $m(k_x,k_y,k_z) = m + \cos k_x + \cos k_y + \cos k_z$ and m controls the bulk gap, and hence the topological phase. The matrices Γ^μ satisfy a Clifford algebra, and are given by $\Gamma^0 = \tau^x s^0$, $\Gamma^x = \tau^y s^0$, $\Gamma^y = \tau^z s^x$, $\Gamma^z = \tau^z s^z$, and $\Gamma^5 = \tau^z s^y$, where the zeroth components τ^0 and s^0 are identity matrices. We can take τ to be an orbital degree of freedom and s is spin; hence the time-reversal operator is $\mathcal{T} = is^yK$ where K is complex conjugation. Further, this model has mirror symmetries along the i-th directions with $\mathcal{M}_i = \Gamma^i\Gamma^5$ where $i = x, y, z$, and importantly $\mathcal{M}_i^2 = -1$. For example, we have $\mathcal{M}_z H_{\rm TI}(k_x,k_y,k_z)\mathcal{M}_z^{-1} = H_{\rm TI}(k_x,k_y,-k_z)$

To introduce a lattice model of the TCI, let us strictly enforce $\mathcal{M}_z$, and add an additional flavor degree of freedom σ^μ to the TI model (2). We will start with a block diagonal form, $H^{(0)}_{\rm TCI} = \sigma^0 \otimes H_{\rm TI}$. The topological phases and surface states of $H^{(0)}_{\rm TCI}$ are determined by m. Without loss generality, we consider a case where $-3 < m < -1$; in this case there are two Dirac nodes (one for each copy) centered at the Γ-point on any surface (see Supplementary Material (SM) Sec. IIIA). $\mathcal{T}$-symmetry enforces $C_{+i}(\Lambda) = -C_{-i}(\Lambda)$, and this model has $C_M(0) = 2, C_M(\pi) = 0$, and $\mathcal{C}_M = 2$.

To produce our phenomena of interest various $\mathcal{M}_z$ preserving perturbations should be added to $H^{(0)}_{\rm TCI}$. [38] Including some such perturbations we can write down a more generic lattice model for the TCI :

$$H_{\rm TCI} = \sin k_x\sigma^0\Gamma^x + (\sin k_y\sigma^0 + b_y\sigma^y)\Gamma^y + \sin k_z\sigma^0\Gamma^z - (m + \cos k_x + \cos k_y + \cos k_z)\sigma^0\Gamma^0 + b_0\sigma^y, \qquad (3)$$

where tensor products are implicit, and we will omit σ^0 from now on for compactness. One can verify that the Hamiltonian (3) is invariant under $\mathcal{M}_z$ and $\mathcal{T}$ (when $b_0 = 0$). One can also introduce b_x and b_z terms that couple to the Hamiltonian in a similar fashion to b_y, and will fill out the entire $b_\mu = (b_0, b_x, b_y, b_z)$ field. Specific mirror symmetries will enforce some entries to be zero, for example $\mathcal{M}_z$ enforces $b_z = 0$. We have left out a non-zero b_x, and some other possible $\mathcal{M}_z$ and $\mathcal{T}$-invariant terms since we will usually specialize to a particular surface ($\hat{n} = \hat{x}$) for convenience, and these additional terms, when small, will not impact our analysis. We note that b_0 breaks time reversal, but not mirror, and we include it in the Hamiltonian because it leads to an interesting EM response contribution. We show in the SM Sec. IIIA that b_0 and b_y move the zero-energy Dirac nodes in the surface BZ from the Γ-point to $(E, k_y, k_z) = (\pm b_0, \pm b_y, 0)$, which, from Eq. (1), is exactly what we need to generate a non-vanishing EM response.

Electromagnetic response.— For our choice of m the TCI Hamiltonian (3) is naturally expanded in the continuum limit around the Γ-point. For $b_0 = b_y = 0$, the continuum Hamiltonian has two identical copies, each with eigenvalue $\sigma^y = \pm 1$ [39] given by

$$H^{(a)} = k_x\Gamma^x + k_y\Gamma^y + k_z\Gamma^z + m'\cos\theta^{(a)}\Gamma^0 + m'\sin\theta^{(a)}\Gamma^5 \qquad (4)$$

where $m' > 0$, $a = 1, 2$ corresponds to the two TI sectors with $\sigma^y = \pm 1$, and we have introduced a new angle parameter $\theta^{(a)}$ for each TI block. Under mirror symmetry $\mathcal{M}_z = \Gamma^z\Gamma^5$, the Hamiltonian satisfies: $\mathcal{M}_z H^{(a)}(k_x, k_y, k_z, \theta^{(a)})\mathcal{M}_z^{-1} = H^{(a)}(k_x, k_y, -k_z, -\theta^{(a)})$. Thus, mirror symmetry enforces $\theta^{(a)}$ to take quantized values of 0 or π. Indeed, our lattice model (3) maintains $\theta^{(a)} = \pi$ throughout the mTCI phase with $\mathcal{C}_M = 2$.

The topological magnetoelectric response [3, 5, 6] of such a system, which is obtained by gapping the surface Dirac nodes with a $\mathcal{T}$-breaking mass, is trivial since we have two copies of the usual TI. However, we now show that there is a response characteristic of a mTCI, once a $\mathcal{M}_z$-breaking mass term is added instead. To calculate the response in the continuum limit we couple each of the continuum Hamiltonians to its own gauge field $A_\mu^{(a)}$ via $\mathbf{k} \to \mathbf{k} + \mathbf{A}^{(a)}$. A diagrammatic calculation similar to those in Refs. 3 and 40 shows that

$$S[A_\mu^{(a)}] = \frac{1}{32\pi^2}\int d^4x\, \theta^{(a)}(x)\epsilon^{\mu\nu\rho\sigma}F_{\mu\nu}^{(a)}F_{\rho\sigma}^{(a)} \tag{5}$$

where $F_{\mu\nu}^{(a)} = \partial_\mu A_\nu^{(a)} - \partial_\nu A_\mu^{(a)}$ is the curvature associated with the gauge field $A_\mu^{(a)}$. The symmetric combination of the gauge fields $A_\mu^{(1)}$ and $A_\mu^{(2)}$ represents the usual EM field A_μ, while the antisymmetric combination generates the energy-momentum separation of the Dirac nodes b_μ, i.e., $eA_\mu = \frac{1}{2}(A_\mu^{(1)} + A_\mu^{(2)}), b_\mu = \frac{1}{2}(A_\mu^{(1)} - A_\mu^{(2)})$. Thus, the total effective response action is given by:

$$\begin{aligned} S[A, b] = \frac{1}{32\pi^2}\int d^4x\, \epsilon^{\mu\nu\rho\sigma}\Big[e^2(\theta^{(1)} + \theta^{(2)})F_{\mu\nu}F_{\rho\sigma} \\ + 2e(\theta^{(1)} - \theta^{(2)})f_{\mu\nu}F_{\rho\sigma} + (\theta^{(1)} + \theta^{(2)})f_{\mu\nu}f_{\rho\sigma}\Big] \end{aligned} \tag{6}$$

where $f_{\mu\nu} = \partial_\mu b_\nu - \partial_\nu b_\mu$ is the curvature of the b_μ. The first (topological magnetoelectric effect) and second terms (the mTCI response of interest) both generate EM observables, though the former has a trivial/doubled coefficient. The current and charge responses depend on changes of the $\theta^{(a)}$ which naturally appear at surfaces, and with signs determined by symmetry breaking mass terms on the surface. A $\mathcal{T}$-breaking mass $m_R\Gamma^5$, similar to that for a TI [3], will generate $\Delta\theta^{(1)} = \Delta\theta^{(2)}$, while a $\mathcal{M}_z$-breaking but $\mathcal{T}$-preserving mass $m_A\sigma^y\Gamma^5$ will generate $\Delta\theta^{(1)} = -\Delta\theta^{(2)}$. The former will generate a (trivial) magnetoelectric response, while the latter will generate the mixed response:

$$S[A, b] = \frac{e}{8\pi^2}\int d^4x\, \Theta(x)\epsilon^{\mu\nu\rho\sigma}f_{\mu\nu}F_{\rho\sigma}, \tag{7}$$

where $\Theta(x) \equiv \theta^{(1)}(x) = -\theta^{(2)}(x)$. For our model we need to introduce the mass term $m_A\sigma^y\Gamma^5$. As noted, the preservation of $\mathcal{T}$ ensures the first term of Eq. (6), a surface Hall effect, vanishes. The sign of the m_A term also fixes the sign of $\Theta = \pi\,\mathrm{sgn}(m_A)$. The same effective action can also be derived in a direct diagrammatic calculation by evaluating the diagram in Fig. 2 of the SM.

Let us illustrate the physical consequences of Eq. 7. The surface of the mTCI can be thought of as a domain wall of $\Theta = \Theta(\vec{x})$ where Θ changes from π to 0 traversing from the mTCI to vacuum. The effective action now reduces to a response localized at the Θ domain wall: $S_{\mathrm{TCI}} = e\,\mathrm{sgn}(m_A)/(4\pi)\int_{\mathrm{surf}} d^3x\epsilon^{\mu\nu\rho}f_{\mu\nu}A_\rho$. Taking a derivative of the effective action with respect to A_μ, i.e., $j^\mu = \delta S/\delta A_\mu$, we obtain the responses:

$$\begin{aligned} j^0{}_{\mathrm{surf}} &= -\frac{e\,\mathrm{sgn}\,m_A}{2\pi}\partial_z b_y, \quad j^z_{\mathrm{surf}} = -\frac{e\,\mathrm{sgn}\,m_A}{2\pi}\partial_0 b_y, \\ j^y{}_{\mathrm{surf}} &= \frac{e\,\mathrm{sgn}\,m_A}{2\pi}\partial_z b_0. \end{aligned} \tag{8}$$

These equations are analogs of the Streda formula and Ohm's law for a Hall current, where $\partial_z b_y$, $\partial_0 b_y$, and $\partial_z b_0$ are the "magnetic field" and "electric field" of the 1-form b_μ. The first equation of (8) indicates that additional charge density is bound at a flux/vortex core of $\vec{b}$. For a domain wall $b_y = |b_y|\,\mathrm{sgn}\,z$ on the yz-surface of the TCI, which has a "magnetic flux" of $\vec{b}$, Eq. (8) predicts that there exists a charge density of $j^0 = e|b_y|\,\mathrm{sgn}(m_A)/\pi$ trapped at the center of the domain wall. Macroscopically these responses arise from the half quantum Hall effect of each surface Dirac cone. They effectively see opposite electric and magnetic fields, but have opposite masses from the mirror-breaking m_A. Hence, their responses add and do not cancel. The defect structure that generates this response is illustrated for this case in Fig. 2. At the end we discuss the physical setup needed to experimentally probe this response.

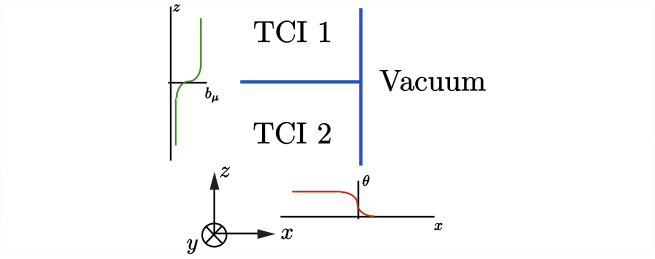

FIG. 2. An illustration showing the kind of domain wall that can probe the response derived in Eq. 7. There is an interface between the TCI and the vacuum at $x = 0$ and an interface between two TCIs with different b_μ at $z = 0$. The quantities b_0, b_y naturally form a domain wall in the x direction at $z = 0$.

These results are based on the particular lattice model (3). However, they hold for any model with $\mathcal{C}_M = C_M(0) + C_M(\pi) = 2$. We show in the SM Sec. II that for a system with $\mathcal{M}_z$ and $\mathcal{T}$ (or even with weakly broken $\mathcal{T}$), $\mathcal{C}_M = 2$ necessarily gives rise to two stable Dirac cones, and thus, upon the introduction of proper mirror-breaking mass terms, the response is described by Eq. (8)

(see Ref. 41 for a discussion of the usual magnetoelectric response for $\mathcal{C}_M = 2$ systems).

For higher $\mathcal{C}_M = N$, there exist N stable surface Dirac nodes, and in principle more complex TCI responses can be obtained, but we leave discussion of those for future work (see Ref. 36 for some related examples in 2D DSMs). For cases with $\mathcal{C}_M = 0$, the surface Dirac cones can be gapped without breaking $\mathcal{M}_z$. However, if the bulk band inversions are at different k-points, then on certain surfaces the two Dirac cones can be located at different locations in the surface BZ. In this case gapping the Dirac cones, when mirror is preserved, requires breaking translational symmetry. By analogy with a weak TI [42, 43], we dub the system with surface Dirac nodes protected by $\mathcal{M}_z$ and translational symmetry a weak mTCI. When translation symmetry is intact, a weak mTCI can have a response (8) on certain surfaces with mirror symmetry, but not necessarily all of them.

Microscopic origin of the response.— Eq. (8) is obtained from the continuum limit. However, from Eq. (3) we see $b_y\sigma^y$ couples to the system like a gauge field *only* in the continuum limit, i.e., when b_y is small. To obtain a complete picture, it is useful to verify the response from a microscopic lattice calculation.

From the TCI lattice model Eq. (3), we first solve for the surface Dirac states on the boundary of a mTCI ($x < 0$) with the vacuum ($x > 0$). The surface Dirac cones at $x = 0$ are given by

$$H_{2\mathrm{D}} = -(\sin k_y + b_y\sigma^y)s^x - \sin(k_z)s^z - m_A s^y\sigma^y, \quad (9)$$

where m_A is the mirror symmetry breaking mass, and the momentum range over which H_{2D} is valid is given by (see SM Sec. IIIB) $|m - 1 + \cos k_y + \cos k_z| < 1$. In the continuum limit where $|b_y|$ is small, we can drop the sine in Eq. (9) and neglect the upper cutoff for $k_{y,z}$. Next, for the non-uniform b_y with a domain wall $b_y(z) = |b_{y0}|\,\mathrm{sgn}\, z$, the solution of Eq. (9) is given by

$$\Psi(x = 0, k_y, z) = \exp\left\{-\int_0^z [k_y\sigma^y + b_y(z')]dz'\right\}\Psi_0(k_y), \quad (10)$$

where $\Psi_0(k_y)$ satisfies $s^y\sigma^y\Psi_0(k_y) = -1$. Eq. (10) describes *two* bound states at each k_y, corresponding to the two eigenvalues of σ^y, both localized in the z-direction at the zero of the integrand of the exponent. Since b_y ranges from $-|b_{y0}|$ to $|b_{y0}|$, only states for which $|k_y| < |b_{y0}|$ have bound state solutions. Therefore, the total number of bound states is $2 \times 2|b_{y0}|/(2\pi/L_y)$. For a finite system, the surface $x = 0$ will also have an opposite domain wall with $b_y(z) = -|b_{y0}|\,\mathrm{sgn}\, z$. There exist the same number of bound states at the opposite domain wall with $s^y\sigma^y = 1$. With a small but finite m_A, the states localized at opposite domain walls are split away from zero energy and can be unambiguously filled (all states on one domain wall are filled). Due to the usual arguments [44], each state generates a localized charge $-\frac{e}{2}\,\mathrm{sgn}\, m_A$. Therefore we find that the bound state charge density is $j^0 = -e|b_{y0}|\,\mathrm{sgn}(m_A)/\pi$, and is in agreement with Eq. (8). We note that to see this response, we only need to break mirror symmetry with an infinitesimal mass term, while time reversal symmetry is intact.

For a larger magnitude of the domain wall $|b_{y0}|$, the charge response can deviate from the prediction from Eq. (8) and become non-universal, but this happens only with a gap closing transition in the bulk. To this end, for a sufficiently small $|b_{y0}|$, the Dirac nodes given by Eq. (9) simply get shifted. However, depending on the momentum range of validity of $H_{2\mathrm{D}}$, a larger value of $|b_{y0}|$ can either eliminate the Dirac nodes or introduce additional Dirac nodes that can gap out each original one. In both cases, there is a gap closing in the bulk which indicates a transition from a mTCI to a trivial insulator. We show in the SM Sec. III that, as long as the bulk gap does not close, the response (8) from the continuum model remains *exact* even in the lattice model. However for the cases when a large b_y eliminates or cancels the original Dirac nodes on the two sides of the domain wall, the charge density bound at the domain wall becomes non-universal.

Implication for experiments.— As discussed above, the universal bulk contribution to the topological magneto-electric effect [3, 5, 6] is absent in a TCI; the Faraday effect and Kerr angles are non-universal when TR is explicitly and infinitesimally broken. However, our predicted response in Eq. (8) can be directly detected in other experiments, which requires engineering a domain wall or time gradient of the b_μ field, i.e., the momentum/energy displacement of the Dirac nodes. The surface Dirac nodes of a TCI can be moved in $\mathbf{k}$-space via compression or dilation strains [46]. For SnTe, the surface Dirac nodes perpendicular to the (001) direction arise at $\pm\mathbf{k}_1, \pm\mathbf{k}_2$ and are protected by mirror symmetry along (110) and $(1\bar{1}0)$ axes, and are related by a C_4 rotation. With Isotropic compression or dilation, b_i's for both pairs of Dirac nodes increase or decrease. With uniaxial compression or stretching that breaks the C_4 symmetry, $b_{i,1}$ increases while $b_{i,2}$ decreases, or vice versa. A spatially inhomogeneous compression/dilation can thus generate the domain wall structure. A temporal gradient of b can be generated by surface acoustic waves produced by electromagnetically stimulating a piezo-electric layer deposited on the surface. The mass terms of the surface Dirac fermions can be generated [32, 47] through structural distortions where the atoms are displaced. After setting up the spatially-varying or time-dependent b_μ the localized charges can be detected by Scanning Tunneling Microscopy (STM) [48, 49] or the Scanning Single Electron Transistor Microscopy (SSETM) [50], while surface currents can be observed by a SQUID magnetometer.

We acknowledge useful discussions with Onkar Parrikar, Vatsal Dwivedi, Awadhesh Narayan and Victor Chua. STR and TLH are supported by the ONR YIP Award N00014-15-1-2383. YW is supported by the Gordon and Betty Moore Foundation's EPiQS Initiative through Grant No. GBMF4305 at the University of Illinois.

[1] D. J. Thouless, M. Kohmoto, M. P. Nightingale, and M. den Nijs, Phys. Rev. Lett. **49**, 405 (1982).
[2] S. Ryu, A. P. Schnyder, A. Furusaki, and A. W. Ludwig, New J. Phys. **12**, 065010 (2010).
[3] X.-L. Qi, T. L. Hughes, and S.-C. Zhang, Phys. Rev. B **78**, 195424 (2008).
[4] A. Kitaev, in *AIP Conference Proceedings*, Vol. 1134 (2009).
[5] A. M. Essin, J. E. Moore, and D. Vanderbilt, Phys. Rev. Lett. **102**, 146805 (2009).
[6] V. Dziom, A. Shuvaev, A. Pimenov, G. Astakhov, C. Ames, K. Bendias, J. Böttcher, G. Tkachov, E. Hankiewicz, C. Brüne, *et al.*, arXiv:1603.05482 (2016).
[7] C. L. Kane and E. J. Mele, Phys. Rev. Lett. **95**, 226801 (2005).
[8] B. A. Bernevig, T. L. Hughes, and S.-C. Zhang, Science **314**, 1757 (2006).
[9] M. König, H. Buhmann, L. W. Molenkamp, T. Hughes, C.-X. Liu, X.-L. Qi, and S.-C. Zhang, Journal of the Physical Society of Japan **77** (2008).
[10] D. Hsieh, D. Qian, L. Wray, Y. Xia, Y. S. Hor, R. J. Cava, and M. Z. Hasan, Nature **452**, 970 (2008).
[11] J. Moore, Nat. Phys. **5**, 378 (2009).
[12] Y. Xia, D. Qian, D. Hsieh, L. Wray, A. Pal, H. Lin, A. Bansil, D. Grauer, Y. Hor, R. Cava, *et al.*, Nat. Phys. **5**, 398 (2009).
[13] T. Zhang, P. Cheng, X. Chen, J.-F. Jia, X. Ma, K. He, L. Wang, H. Zhang, X. Dai, Z. Fang, *et al.*, Phys. Rev. Lett. **103**, 266803 (2009).
[14] C.-Z. Chang, J. Zhang, X. Feng, J. Shen, Z. Zhang, M. Guo, K. Li, Y. Ou, P. Wei, L.-L. Wang, *et al.*, Science **340**, 167 (2013).
[15] L. Fu and C. L. Kane, Phys. Rev. B **76**, 045302 (2007).
[16] J. C. Y. Teo, L. Fu, and C. L. Kane, Phys. Rev. B **78**, 045426 (2008).
[17] L. Fu, Phys. Rev. Lett. **106**, 106802 (2011).
[18] T. L. Hughes, E. Prodan, and B. A. Bernevig, Phys. Rev. B **83**, 245132 (2011).
[19] A. M. Turner, Y. Zhang, R. S. Mong, and A. Vishwanath, Physical Review B **85**, 165120 (2012).
[20] C. Fang, M. J. Gilbert, and B. A. Bernevig, Phys. Rev. B **86**, 115112 (2012).
[21] J. C. Teo and T. L. Hughes, Phys. Rev. Lett. **111**, 047006 (2013).
[22] R.-J. Slager, A. Mesaros, V. Juričić, and J. Zaanen, Nat. Phys. **9**, 98 (2012).
[23] W. A. Benalcazar, J. C. Teo, and T. L. Hughes, arXiv preprint arXiv:1311.0496 (2013).
[24] T. Morimoto and A. Furusaki, Phys. Rev. B **88**, 125129 (2013).
[25] C.-K. Chiu, H. Yao, and S. Ryu, Phys. Rev. B **88**, 075142 (2013).
[26] C. Fang, M. J. Gilbert, and B. A. Bernevig, Phys. Rev. B **87**, 035119 (2013).
[27] T. L. Hughes, H. Yao, and X.-L. Qi, arXiv:1303.1539 (2013).
[28] Y. Ueno, A. Yamakage, Y. Tanaka, and M. Sato, Phys. Rev. Lett. **111**, 087002 (2013).
[29] F. Zhang, C. Kane, and E. Mele, Phys. Rev. Lett. **111**, 056403 (2013).
[30] P. Jadaun, D. Xiao, Q. Niu, and S. K. Banerjee, Phys. Rev. B **88**, 085110 (2013).
[31] R.-J. Slager, A. Mesaros, V. Juričić, and J. Zaanen, Nature Physics **9**, 98 (2013).
[32] T. H. Hsieh, H. Lin, J. Liu, W. Duan, A. Bansil, and L. Fu, Nat. Comm. **3**, 982 (2012).
[33] Y. Tanaka, Z. Ren, T. Sato, K. Nakayama, S. Souma, T. Takahashi, K. Segawa, and Y. Ando, Nat. Phys. **8**, 800 (2012).
[34] S.-Y. Xu, C. Liu, N. Alidoust, M. Neupane, D. Qian, I. Belopolski, J. Denlinger, Y. Wang, H. Lin, L. Wray, *et al.*, Nat. Comm. **3**, 1192 (2012).
[35] P. Dziawa, B. Kowalski, K. Dybko, R. Buczko, A. Szczerbakow, M. Szot, E. Łusakowska, T. Balasubramanian, B. M. Wojek, M. Berntsen, *et al.*, Nature materials **11**, 1023 (2012).
[36] S. T. Ramamurthy and T. L. Hughes, Phys. Rev. B **92**, 085105 (2015).
[37] B. A. Bernevig, *Topological Insulators and Topological Superconductors* (Princeton University Press, 2013).
[38] We have continued using $\mathcal{T} = is^yK$ in the doubled TCI model as well. This is a basis choice that affects the necessity of using σ^y instead of σ^z in coupling b_μ to the model. However, one could use σ^z in the coupling instead, and use $\mathcal{T} = i\sigma^x s^y K$ as the definition of time-reversal operator acting on the Bloch Hamiltonian.
[39] Note that, while it is more conventional to refer to $\sigma^z = \pm 1$ as two copies, we have chosen $\sigma^y = \pm 1$. This is merely a basis choice, and we have done so to preserve time-reversal symmetry, as the real materials examples do.
[40] C. G. Callan Jr and J. A. Harvey, Nuclear Physics B **250**, 427 (1985).
[41] D. Varjas, F. de Juan, and Y.-M. Lu, Physical Review B **92**, 195116 (2015).
[42] L. Fu, C. L. Kane, and E. J. Mele, Phys. Rev. Lett. **98**, 106803 (2007).
[43] J. E. Moore and L. Balents, Phys. Rev. B **75**, 121306(R) (2007).
[44] R. Jackiw and C. Rebbi, Phys. Rev. D **13**, 3398 (1976).
[45] W. Cho and S. A. Kivelson, Phys. Rev. Lett. **116**, 093903 (2016).
[46] E. Tang and L. Fu, Nature Physics **10**, 964 (2014).
[47] M. Drüppel, P. Krüger, and M. Rohlfing, Phys. Rev. B **90**, 155312 (2014).
[48] G. Binnig and H. Rohrer, Surface science **126**, 236 (1983).
[49] P. Sessi, D. Di Sante, A. Szczerbakow, F. Glott, S. Wilfert, H. Schmidt, T. Bathon, P. Dziawa, M. Greiter, T. Neupert, G. Sangiovanni, T. Story, R. Thomale, and M. Bode, Science **354**, 1269 (2016), http://science.sciencemag.org/content/354/6317/1269.full.pdf.
[50] M. Yoo, T. Fulton, H. Hess, R. Willett, L. Dunkleberger, R. Chichester, L. Pfeiffer, and K. West, Science **276**, 579 (1997).